Korean J. Chem. Eng., **29**(5), 621-626 (2012)
DOI: 10.1007/s11814-011-0225-z

Development of non-precious oxygen reduction reaction catalyst for polymer electrolyte membrane fuel cells based on substituted cobalt porphyrins

Singaram Vengatesan, Eunae Cho†, and In-Hwan Oh

Center for Fuel Cell Research, Korea Institute of Science and Technology, 39-1, Hawolgok-dong, P. O. Box 131, Cheongryang, Seongbuk-gu, Seoul 136-791, Korea
(*Received 28 June 2011 • accepted 27 August 2011*)

Abstract–Active and stable cobalt-based non-precious metal catalysts for the oxygen reduction reaction (ORR) in PEM fuel cells were developed through high-temperature pyrolysis of metal-porphyrins supported on carbon. The roles of substituted porphyrins, carbon support, and catalyst loading on ORR activity were studied using rotating disc electrode (RDE) measurements. It was observed that the carbon support plays a major role in improving the catalytic activity. The results showed that among the supported catalysts, the homemade mesocarbon-supported cobalt-porphyrin catalyst with 20 wt% loading displayed higher ORR activity; the cell performance showed maximum current density of 1.1 A cm^{-2} at 0.13 V in H_2/O_2 fuel cells.

Key words: Non-precious Metal Catalyst, Metal-porphyrin, ORR Activity, Rotating Disc Electrode, Polymer Electrolyte Membrane Fuel Cells

INTRODUCTION

Polymer electrolyte membrane fuel cells (PEMFCs) are considered future energy sources for transportation and stationary applications [1,2]. Although enormous achievements have been made in this area, the realization of fuel cell technology for commercial usage is still in its nascent state. The challenge of the research and technological development of fuel cells, especially of PEMFCs, lies in the catalytic materials for both the anode and cathode. Pt and Pt alloys are widely used as anode and cathode materials for their excellent activity and high stability at PEMFC conditions [3-5]. Despite a cathodic overpotential loss of 20%, Pt and its alloys are still preferred because of their high resistance against corrosion in acidic media. However, the high cost and low abundance of these precious metals obstruct successful commercialization of fuel cell technology [6]. Though the loading of platinum metal or alloys applied to electrodes has been suppressed to only several milligrams, the question of replacement of these expensive metals by other active low cost materials remains unresolved.

Work towards the development of non-noble metal catalysts for fuel cells has greatly intensified in recent years [7-13]. Among the non-noble metal based catalysts, transition metal oxides (e.g., perovskitic LaSrCo oxides) [12], chalcogenides [13], and transition metal-macrocycles) [9] have been considered as possible fuel cell catalysts. The class of non-precious metal catalysts that has attracted the most attention over the years is pyrolyzed transition metal-macrocycles that have porphyrin or phthalocyanine chelating ligands [14, 15]. It is assumed that the ligands on the central metal ion stabilize the metal ion through inductive and mesomeric effects and are attributed to oxygen reduction in acidic media [15]. Moreover, it is reported that heat-treatment of metal-macrocycles provides increased activity and stability to the catalytic system [16-18]. Among the metal macrocycles, iron (Fe) and cobalt (Co) porphyrins are found to be most active and stable ORR catalysts [19]. According to the literature [15,20], Fe-based catalysts showed higher activity but lower stability than Co-based catalysts. It is believed that Fe catalysts favor the $4e^-$ pathway, in which the oxygen is directly reduced to water. Though the ORR activity of these catalysts has been explored, the actual chemical structure of the catalytic active sites and their subsequent mechanism is still unclear.

To improve the catalyst activity and stability of M-N catalysts, a variety of approaches have been explored, such as using different N-containing macrocycles and metal precursors, exploring different carbon supports, and developing various heat treatment strategies [21-25]. It is believed that N-containing macrocycles play a critical role in activity, and addition of functional groups or substituents to a macrocycle could modify its chemical as well as electrochemical properties and functionalities. Depending on the nature and position of functional groups introduced onto the macrocycles, the catalytic activity as well as the associated reaction mechanisms can be changed significantly. In addition, carbon support also plays an important role in improving the activity and stability of heat-treated metal macrocycles [26]. The intrinsic properties of carbon supports, such as porosity, surface area, electrical conductivity, and crystallinity, would be the factors responsible for modification of the ORR activity. However, while remarkable progress has been made in non-noble metal based catalysts, none of the reported catalysts have reached the level of a Pt-based catalyst.

Thus, in this work, an attempt was made to study and improve the catalytic activity of cobalt-porphyrin based non-precious metal catalysts. For that, the ORR activities of heat-treated cobalt-porphyrins as functions of different peripheral substituents were evaluated using rotating disc electrode measurement. In addition, the role of carbon support on ORR activity was studied using carbon supports with different surface characteristics. The catalyst loading on

†To whom correspondence should be addressed.
E-mail: eacho@kist.re.kr

carbon support was varied and optimized. Finally, the catalyst performance was also evaluated in a single PEMFC.

EXPERIMENTAL

1. Preparation of Carbon Supported Co-porphyrin Catalysts

Cobalt-porphyrin was prepared on carbon support by the impregnation method [27]. Anhydrous cobalt acetate was dissolved in methanol and sonicated for 30 min. Carbon powder was added to the metal solution, and the mixture was ultrasonicated for another 1 h. Next, the methanol was evaporated using a rotavapor, and the mixture was dried at 60 °C in a vacuum oven. The porphyrin ligand (Co/porphyrin=1 : 1 molar ratio) was dissolved in concentrated formic acid in an ultrasonic bath for 30 min, and the carbon mixture containing the cobalt metal was added gradually and stirred for another 1 h. The formic acid was evaporated using a rotavapor, and the mixture was dried overnight at 80 °C in a vacuum oven. The dried mixture was homogenized in a mixer and the sample was heat-treated at 800 °C in a horizontal quartz tube under a continuous flow of nitrogen for 3 h. The reactor was cooled until it reached ambient temperature, and the catalyst was homogenized in a mixer.

Following the above procedure, various heat-treated Co-porphyrin catalysts were prepared by changing the porphyrin ligands and carbon supports. The substituted porphyrin ligands used in this study are shown in Fig. 1. The ligands are *meso-tetra phenyl porphine* (TPP), *meso-tetramethoxy phenyl porphine* (TMPP), *meso-tetra (3,5-di-tert-butyl phenyl) porphine* (TBPP), *meso-tetra (2,3,4,5,6-penta-flouro phenyl) porphine* (TFPP), *meso-tetra (4-carboxy phenyl) porphine tetramethyl ester* (TMCP), and *meso-tetra (4-pyridyl) porphine* (TPyP). The carbon supports used were Vulcan XC72R, BP 2000, modified BP 2000, and homemade mesocarbon, where modified BP2000 was prepared by treating the BP2000 carbon with 40% HNO_3 at 80 °C, whereas the homemade mesocarbon was prepared using our previously reported procedure [28].

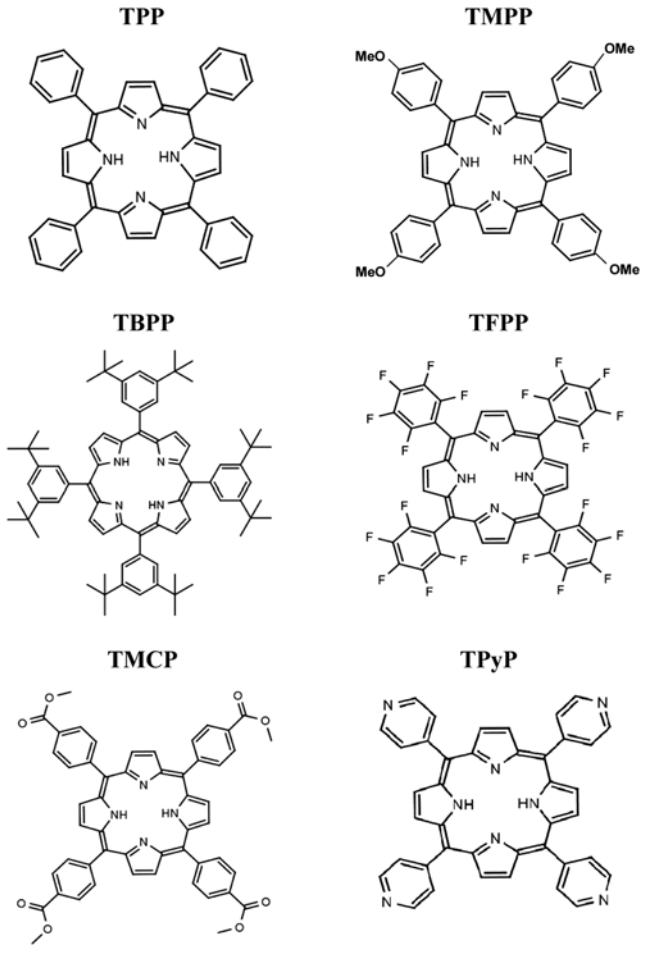

Fig. 1. Chemical structure of different porphyrin ligands.

The surface morphology and composition of catalyst particles on the support was characterized by a Philips CM30 TEM-EDAX analyzer.

2. Preparation of Membrane Electrode Assemblies (MEAs)

The catalyst inks for the electrodes were prepared by mixing carbon-supported catalyst, 5 wt% Nafion solution (DuPont) and isopropyl alcohol (Baker HPLC grade reagent). The catalyst inks were sprayed onto the carbon paper (Toray TGPH-60). The cathode catalyst layer of the MEA had a catalyst loading of 6.0 mg cm^{-2} heat-treated Co-porphyrin/C catalyst, and the anode catalyst layer had a catalyst loading of 0.5 mg cm^{-2} Pt (40 wt% Pt/C, E-Tek Inc.). The MEA was made by keeping a Nafion 112 membrane in between anode and cathode electrodes and hot-pressing at 140 °C at a pressure of 200 kg cm^{-2} for 90 s.

3. CV and RDE (Rotating Disc Electrode) Measurements

The electrochemical properties of non-precious metal catalysts were investigated by CV and RDE analysis. The analyses were performed on a three-electrode cell with glassy carbon (5.0 mm dia.), saturated calomel electrode (SCE), and platinum mesh serving as the working, reference, and counter electrodes. The electrolyte used was 0.5 M sulfuric acid (H_2SO_4) solution. The homemade catalyst was mixed with isopropyl alcohol to make the catalyst slurry. The catalyst slurry was then applied onto the working electrode and dried for several minutes, followed by applying 3 μL of 5 wt% Nafion solution (DuPont Fluoroproducts) onto the catalyst layer. The total catalyst loading on the working electrode was 140 μg cm^{-2}. For comparison, a working electrode with commercial Pt/C - 20 wt% (E-TeK Inc.) was also prepared and evaluated.

4. Analysis of MEA and Single Cell Tests

Single cells were assembled with MEA, Teflon gaskets, and graphite blocks. The active cell area was 10 cm^2 (3.3 cm×3.3 cm). Hydrogen and oxygen were fed to the anode and cathode at a flow rate of 500 cc min^{-1}. The single cell was operated at 70 °C under ambient pressure. The anode and cathode humidifier temperatures were maintained at 70 and 65 °C, respectively. The cell performance was evaluated by measuring the i-V characteristics using an electric load (Daegil electronics, EL50P).

The impedance of the single cells was measured by means of AC impedance spectroscopy. The instrument (Zahner electric IM6) was used in a potentiostatic mode at 0.6 V with an amplitude of 5 mV and the frequency from 10 mHZ to 10 kHZ.

RESULTS AND DISCUSSION

Among the various porphyrin ligands, heat-treated Co-TMPP/C catalyst was chosen for the physical properties such as TEM images and surface analysis. Fig. 2(a) shows the TEM image of heat-treated

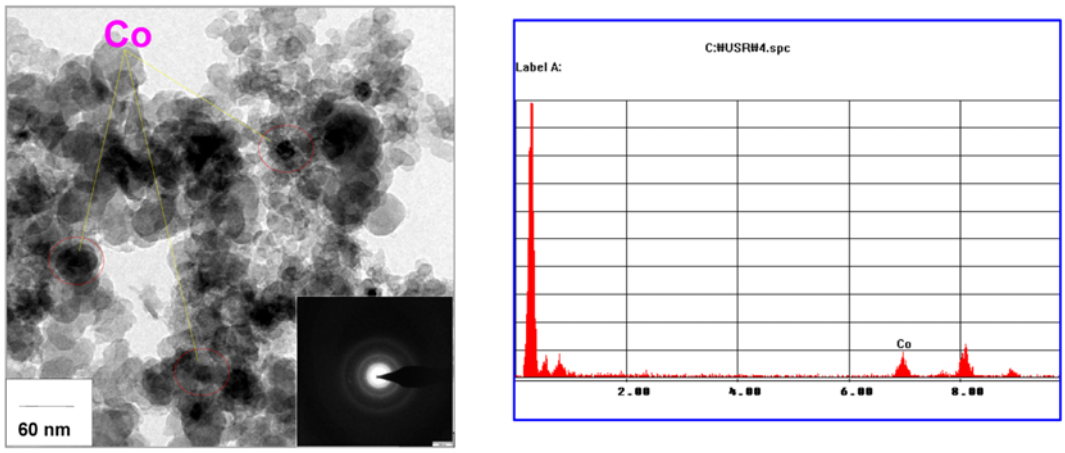

Fig. 2. (a) TEM image; (b) EDAX spectrum of heat-treated Co-TMPP 20 wt% catalyst on Vulcan carbon.

Co-TMPP/C catalyst with 20 wt% metal-porphyrin loading. From the TEM analysis, the cobalt particles are randomly dispersed on the carbon support. The morphology of the catalyst particles shows spherical shape with well defined crystalline pattern (inset). From the figure, the particle size of the cobalt is found to be ~20 nm. It is possible that the original cobalt-porphyrin complex was destroyed during the pyrolysis step and that the cobalt atoms agglomerated. The surface EDAX mapping of the catalyst is illustrated in Fig. 2(b), and it shows the existence of cobalt in the catalyst.

The change in catalytic activity as the macrocycle stabilizes the central metal ion by inductive effects is attributed to the nature of substituents present in the macrocycle. For the electrochemical characterization of cobalt-porphyrin catalysts, CV was conducted in 0.5 M H_2SO_4 under saturated N_2. Fig. 3(a) shows the cyclic voltammograms of the cobalt-porphyrin catalysts with different substituents on the porphyrin ligand. From the CV, no distinct peaks were observed in the potential range for the cobalt-porphyrin catalysts, but the voltammogram shows the features of carbon support. However, for Pt/C coated electrode, characteristic peaks for hydrogen-oxidation and oxygen-reduction are observed. The catalytic activity of cobalt-porphyrin catalysts towards ORR was examined by the polarization of its coated electrode in 0.5 M H_2SO_4 under saturated O_2.

Fig. 3(b) shows the RDE curves of the cobalt-porphyrin catalysts with different substituents on the porphyrin ligand. In RDE, the onset potential indicates the measure of catalyst activity towards the oxygen reduction reaction. From the curves, the onset potential for oxygen reduction slightly decreased as the substituents were introduced onto the TPP ligand, which shows that the substituent groups play a negative role by deactivating the macrocycle during the pyrolysis step. However, the pyridyl substituted porphyrin (TPyP) exhibits slightly higher onset potential for ORR. This might have arisen from the excess nitrogen functionalities present in the pyridyl-substituted porphyrin. As established by Dodelet and co-workers [23,29], nitrogen is a necessary component of the catalyst site in order to form an active catalyst. On other hand, the Pt/C catalyst showed comparatively very high onset potential (>0.87 V) for ORR. Since the onset potential was similar for all porphyrin ligands, TMPP was employed for further investigation.

For supported catalysts, the optimum metal content on the support is very crucial, as it determines the catalytic activity of the catalyst. The optimum metal-porphyrin loading was determined by the nature of the precursors used, the surface properties of the carbon support, and the heat treatment conditions [30,31]. The loading can also affect the degree to which the carbon-support surface is covered, result-

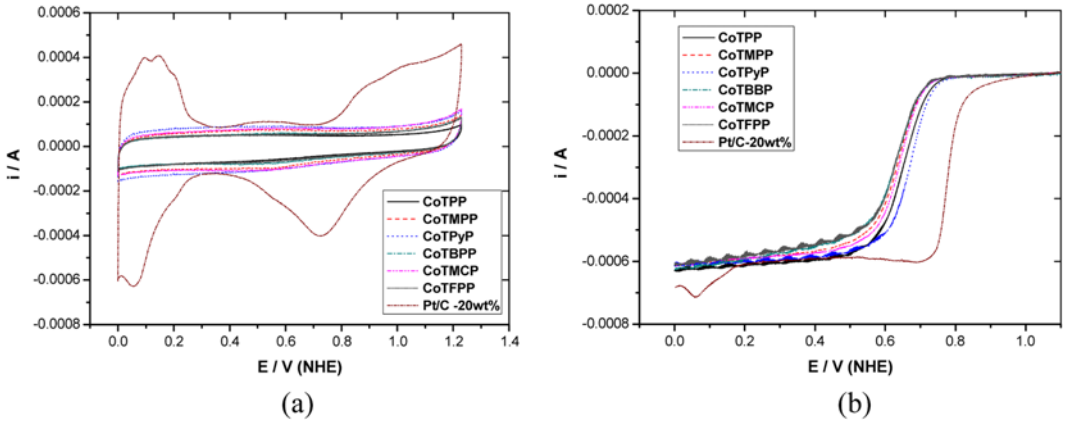

Fig. 3. (a) Cyclic voltammograms; (b) RDE voltammograms of cobalt-porphyrin catalysts with different porphyrin ligands.

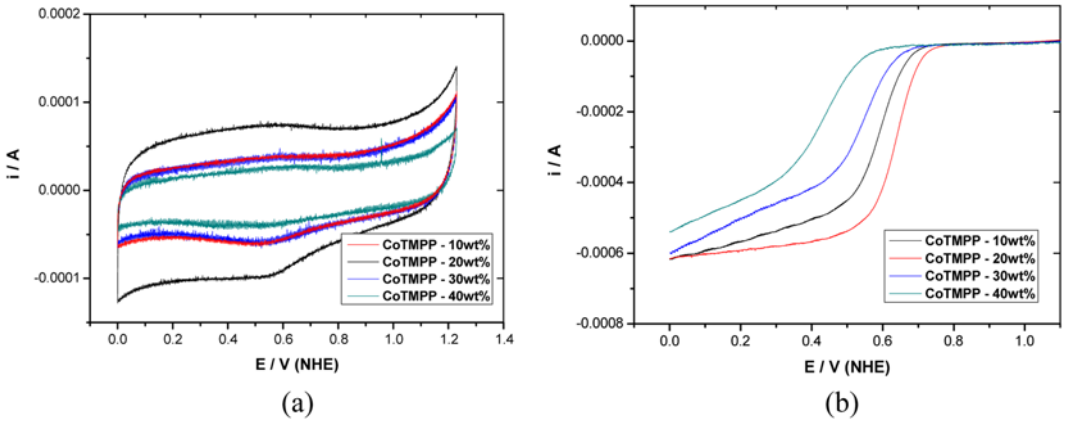

Fig. 4. (a) Cyclic voltammograms; (b) RDE voltammograms of Co-TMPP/C catalysts with different metal-porphyrin loading on Vulcan carbon.

ing in a change in support-specific surface area. Fig. 4(a) shows the cyclic voltammograms of Co-TMPP/C catalysts with different cobalt-porphyrin loadings on the carbon support. From the CV, the curve area increased as the catalyst loading increased from 10 to 20 wt%. However, at 30 wt%, the curve area decreased, drastically decreasing further at 40 wt%. This shows that 20 wt% is the optimum loading of catalyst at which the catalyst particles are well-dispersed while maintaining the specific surface area of the carbon support. The RDE voltammograms shown in Fig. 4(b) exhibited a similar trend to that of CV (Fig. 4(a)). The 20 wt% Co-TMPP loaded catalyst showed the highest onset potential for ORR, and the onset potential decreased as the metal-porphyrin loading was altered up or down from 20 wt%.

Carbon support plays an important role in improving the activity and stability of heat-treated metal macrocycles [26]. In addition, the surface properties of the carbon support have a significant effect on the degree of catalyst dispersion. Fig. 5 shows the CV and RDE curves of Co-TMPP 20 wt% catalyst on various carbon supports. From the CV, the electrochemical double-layer thickness for BP 2000 and mesocarbon-supported catalysts are higher than Vulcan-supported catalyst, which is attributable to the high surface area of the BP200 and mesocarbon supports. However, the RDE curves of these supported catalysts displayed a significant difference in their pattern. Among the supported catalysts, the Vulcan-supported catalyst showed the lowest onset potential (~0.75 V) for ORR. The BP 2000 supported catalyst showed a slight increase in onset potential (~0.77 V), and the modification of BP 2000 carbon support produced a further 10 mV gain in onset potential. The chemical activation of BP 2000 support may produce oxygen-containing functional groups on the support, which in turn assisted the dispersion of the metal complex on the support. Among the catalysts, the mesocarbon-supported Co-TMPP catalyst showed the highest onset potential (~0.8 V) for ORR. Although mesocarbon and BP 2000 have similarly high surface areas, the higher activity of mesocarbon-supported catalyst might be attributed to some additional effect. This observed phenomenon can be explained as follows: as the mesocarbon is prepared by carbonizing the polyaniline precursor, which contains nitrogen functionality, the carbon may acquire excess N from the precursor. Jaouen et al. [25,32] observed that higher N concentration on the support surface could produce better catalytic activity. Following this, some of the researchers also introduced N-containing groups on the carbon surface by carbonizing N-containing compounds, observing good catalytic activity [24,33-35].

Finally, an Fe-TMPP catalyst was also prepared and compared with the Co-TMPP catalyst. Fig. 6 shows the CV and RDE curves of Fe-TMPP and Co-TMPP catalysts with 20 wt% loading on Vulcan support. From the RDE, the Fe-TMPP catalyst showed more positive onset potential for ORR than the Co-TMPP catalyst. This

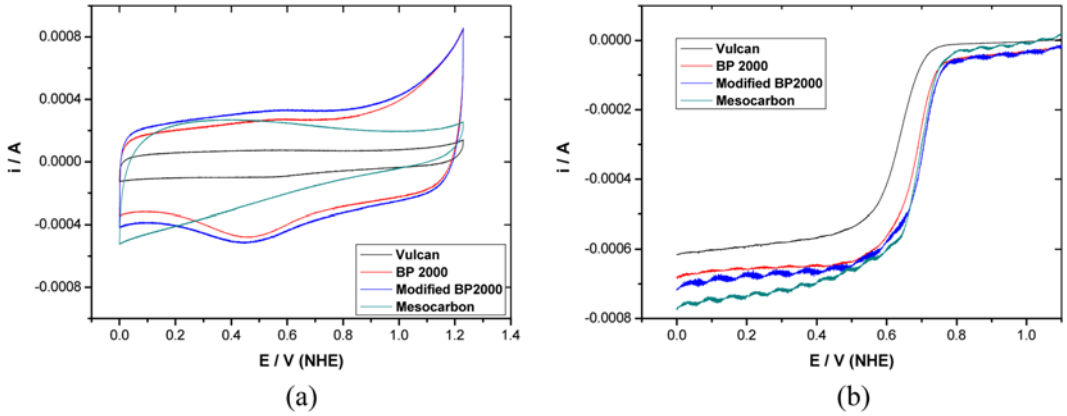

Fig. 5. (a) Cyclic voltammograms; (b) RDE voltammograms of Co-TMPP 20 wt% catalysts on different carbon supports.

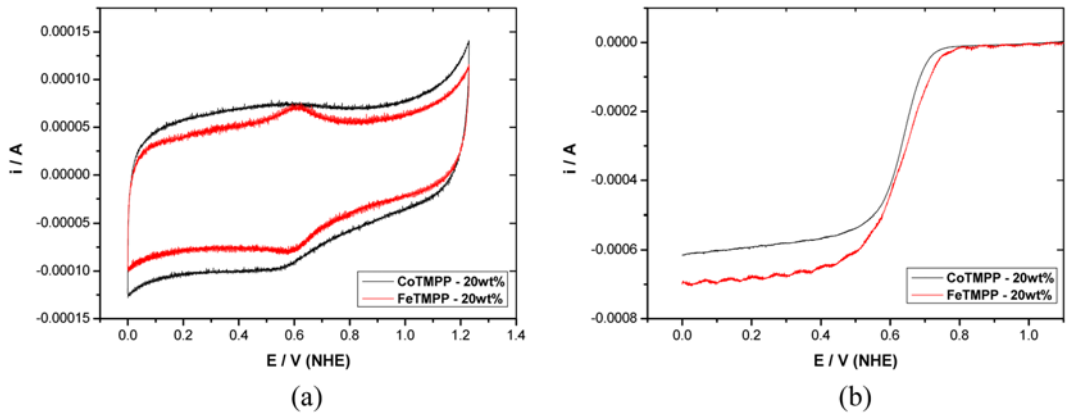

Fig. 6. (a) Cyclic voltammograms; (b) RDE voltammograms of Co-TMPP 20 wt% and Fe-TMPP 20 wt% catalysts.

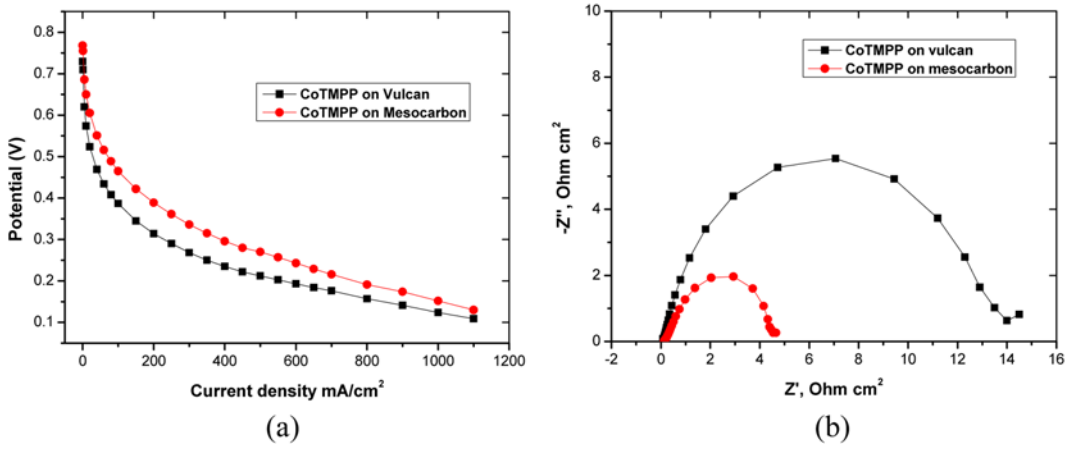

Fig. 7. (a) i-V characteristics; (b) impedance spectra of MEAs using heat-treated Co-porphyrin catalysts. The cathode catalyst loading was 6.0 mg cm^{-2}. Cell temperature was 70 °C and pressure was 1 atm.

confirmed the literature evidence that the Fe-TMPP catalyst is more active towards ORR than the Co-TMPP catalyst [15,20,21].

To evaluate the ORR activity of prepared catalysts at the operational fuel cell conditions, MEAs were fabricated with heat-treated Co-porphyrin/C as cathode catalyst that was reported to be relatively durable under PEMFC conditions [10]. Fig. 7(a) shows the polarization curves of two different MEAs at 70 °C using Co-TMPP on Vulcan support and Co-TMPP on mesocarbon support as cathode catalysts. From the figure, the maximum current density of 1.1 A cm^{-2} was achieved for both MEAs at the cell voltage of around 0.12 V. Between the two catalysts, the mesocarbon-supported Co-TMPP catalyst showed higher performance, especially in the kinetically controlled regime. This is in good agreement with the RDE results, in which the mesocarbon-supported catalyst showed higher ORR onset potential than other catalysts (Fig. 5(b)). Fig. 7(b) shows the impedance spectra of the single cells and displays a large semicircle that reflects the slow kinetics of oxygen reduction upon the catalysts.

CONCLUSIONS

Cobalt-porphyrin based non-noble metal catalysts were prepared by the impregnation method. The role of substituted porphyrin ligands on ORR activity was studied by introducing different substituent groups onto porphyrin ligands. It was observed that the substituted groups deactivate the metal complex during the pyrolysis and reduce its ORR activity. The metal-porphyrin loading on the support varied from 10 to 40 wt%, and the optimum loading was found to be 20 wt%. The influence of carbon support on ORR activity was explored by preparing the catalyst with different carbon supports. Compared with Vulcan-supported catalyst, the catalysts supported on high surface area carbons showed higher ORR activities. The mesocarbon supported catalyst exhibited the highest onset potential (~0.8 V) for ORR, which is mainly attributed to its nitrogen functionality. The results show that the carbon plays a very significant role in improving ORR activity and reveal that the presence of N-functionality on the carbon surface is important for the catalytic activity.

The single-cell performance of MEAs using heat-treated Co-TMPP/C as the cathode catalyst produced the maximum current density of 1.1 A cm^{-2}. Further improvements in ORR activity of these catalysts will make them a potential catalyst for PEMFC.

ACKNOWLEDGEMENT

This work was supported by Energy-Bank Program of Korea Institute of Science and Technology.

REFERENCES

1. S. Srinivasan, R. Mosdale, P. Stevens and C. Yang, *Annu. Rev. Energy Environ*., **24**, 281 (1999).
2. A. J. Appleby and F. R. Foulkes, *Fuel cell handbook*, Van Nostrand Reinhold, New York (1989).
3. P. N. Ross Jr, in: W. Vielstich, A. Lamm, H. A. Gasteiger (Eds.), *Handbook of fuel cells*, Vol. 2, Wiley, Newyork, 465 (2003).
4. E. Antolini, J. R. C. Salgado and E. R. Gonzalez, *J. Power Sources*, **160**, 957 (2006).
5. J. H. Kim, S. M. Choi, S. H. Nam, M. H. Seo, S. H. Choi and W. B. Kim, *Appl. Catal. B: Environ*., **82**, 89 (2008).
6. C. Jaffray, G. Hards, in: W. Vielstich, A. Lamm, H. A. Gasteiger (Eds.), *Handbook of fuel cells*, Vol. 3, Wiley, New York, 509 (2003).
7. B. Wang, *J. Power Sources*, **152**, 1 (2005).
8. L. Zhang, J. Zhang, D. P. Wilkinson and H. Wang, *J. Power Sources*, **156**, 171 (2006).
9. C. W. B. Bezerra, L. Zhang, K. Lee, H. Liu, A. L. B. Marques, E. P. Marques, H. Wang and J. Zhang, *Electrochim. Acta*, **53**, 4937 (2008).
10. R. Bashyam and P. Zelenay, *Nature*, **443**, 63 (2006).
11. V. Nallathambi, J.-W. Lee, S. P. Kumaraguru, G. Wu and B. N. Popov, *J. Power Sources*, **183**, 34 (2008).
12. A. V. Sankarraj, S. Ramakrishnan and C. Shannon, *Langmuir*, **24**, 632 (2008).
13. K. Lee, L. Zhang and J. Zhang, *Electrochem. Commun*., **9**, 1704 (2007).
14. S. Pylypenko, S. Mukherjee, T. S. Olson and P. Atanassov, *Electrochim. Acta*, **53**, 7875 (2008).
15. K. Wiesener, D. Ohms, V. Neumann and R. Franke, *Mater. Chem. Phys*., **22**, 457 (1989).
16. H. Jhanke, M. Schonbron and G. Zimmerman, *Top. Curr. Chem*., **61**, 133 (1976).
17. G. Faubert, G. Lalande, R. Cote, D. Guay, J. P. Dodelet, L. T. Weng, P. Bertrand and G. Denes, *Electrochim. Acta*, **41**, 1689 (1996).
18. M. Bron, S. Fiechter, M. Hilgendorff and P. Bogdannoff, *J. Appl. Electrochem*., **32**, 211 (2002).
19. N. A. Savastenko, V. Bruser, M. Bruser, K. Anklam, S. Kutschera, H. Steffen and A. Schumuhl, *J. Power Sources*, **165**, 24 (2007).
20. H. Alt, M. Binder and G. Sandstede, *J. Catal*., **28**, 8 (1973).
21. D. Ohms, S. Herzog, R, Franke, V. Neumann and K. Wiesener, *J. Power Sources*, **38**, 327 (1992).
22. T. Okada, M. Gokita, M. Yuasa and I. Sekine, *J. Electrochem. Soc*., **145**, 815 (1998).
23. J. Fournier, G. Lalande, R. Cote, D. Guay and J. P. Dodelet, *J. Electrochem. Soc*., **144**, 218 (1997).
24. G. Faubert, R. Cote, J. P. Dodelet, M. Lefevre and P. Bertrand, *Electrchim. Acta*, **44**, 2589 (1999).
25. F. Jaouen, F. Charraterour and J. P. Dodelet, *J. Electrochem. Soc*., **153**, A689 (2006).
26. A. Widelov and R. Larsson, *Electrochim. Acta*, **37**, 187 (1992).
27. Y. Kiros, *Int. J. Electrochem. Sci*., **2**, 285 (2007).
28. S. Vengatesan, H. J. Kim, S. K. Kim, I. H. Oh, S. Y. Lee, E. A. Cho, H. Y. Ha and T. H. Lim, *Electrochim. Acta*, **54**, 856 (2008).
29. G. Lalande, R. Cote, D. Guay, J. P. Dodelet, L. T. Weng and P. Bertand, *Electrochim. Acta*, **42**, 1379 (1997).
30. H. Wang, R. Cote, G. Faubert, D. Guay and J. P. Dodelet, *J. Phys. Chem. B*, **103**, 2589 (1999).
31. M. Bron, J. Radnik, M. F. Erdmann, P. Bogdadoff and S. Fiechter, *J. Electroanal. Chem*., **535**, 113 (2002).
32. F. Jaouen, S. Marcotte, J. P. Dodelet and G. Lindbergh, *J. Phys. Chem. B*, **107**, 1376 (2003).
33. M. Lefevre, J. P. Dodelet and P. Bertrand, *J. Phys. Chem. B*, **106**, 8705 (2002).
34. M. Lefevre and J. P. Dodelet, *Electrochim. Acta*, **48**, 2749 (2003).
35. M. Lefevre, J. P. Dodelet and P. Bertrand, *J. Phys. Chem. B*, **109**, 16718 (2005).